Are biosynthesized nanomaterials toxic for the environment? Effects of perlite and CuO/perlite nanoparticles on unicellular algae *Haematococcus pluvialis*

Borna Ali Babazadeh[1] · Jafar Razeghi [1] · Saeed Jafarirad[2] · Rouhollah Motafakkerazad[1]

Abstract

The properties of nanomaterials such as perlite nanoparticles and their increased application have raised concerns about their probable toxic impacts on the aquatic ecosystems and algae. Here, a novel biochemical synthesis and immobilization of CuO is reported on perlite nanoparticles (CuO/Per-NPs) and its toxic effect on alga has been compared with nanoperlites. This biosynthesis of CuO/Per-NPs performed using phytochemicals of *Haematococcus pluvialis, Sargassum angustifolium, and* walnut leaves in the aqueous extract. The structural, morphological, and colloidal properties of the as-synthesized nanoparticles have been confirmed by various methods. According to the obtained results, the morphology of the synthesized CuO/Per-NPs was spherical with sizes ranging from about 13 to 24 nm. Besides, the effects of Per-NPs and CuO/Per-NPs on unicellular algae *H. pluvialis* were studied. The changes in the amount of chlorophyll *a*, chlorophyll *b*, and Carotenoids in the presence of different concentrations of Per-NPs (25, 50, 100 mg/L) were more than CuO/Per-NPs. Also, decreased growth rate and efficiency of photosystem II confirmed the toxic effects of Per-NPs. However, the toxicity of CuO/Per-NPs appears to be lower than that of Per-NPs, which can be due to the changes in the surface and cationic charge of modified nanoperlit. These changes lead to a decrease in the interaction of nanoparticles with *H. pluvialis* and a reduction in ROS production. Finally, the results of GC-MS used to evaluate volatile compounds, indicated an increase in the number of phenolic compounds in comparison to the control samples in 25, 50, and 100 mg/L treatments of nano-perlite.
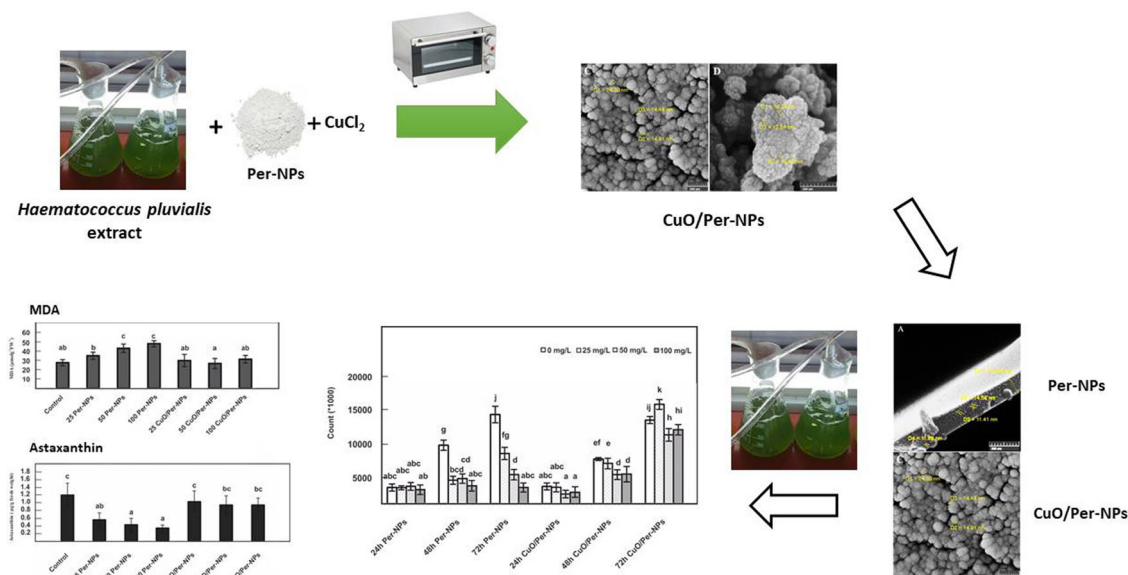
✉ Jafar Razeghi
   jafar_razeghi@tabrizu.ac.ir

✉ Saeed Jafarirad
   jafarirad@tabrizu.ac.ir

1   Department of Plant Sciences, Faculty of Natural Sciences, University of Tabriz, Tabriz, Iran

2   Research institute of bioscience and biotechnology, University of Tabriz, Tabriz, Iran

🖉 Springer

Graphical Abstract

Keywords Metal-oxide nanoparticles · Toxicity · Astaxanthin · Volatile compounds · Microalga · Phytochemical metabolites

Highlights

- The toxicity of biosynthesized CuO/Per-NPs appears to be lower than that of Per-NPs which are used as superabsorbent of heavy metals in water environment.
- Decreasing growth rate and photosystem II efficiency confirmed the toxic effects of Per-NPs on Alga *Haematococcus pluvialis*.
- Lower toxicity effect of CuO/Per-NPs than Per-NPs can be due to the changes in the surface and cationic charge of modified nanoperlit.
- The changes in the surface of modified nanoperlit (CuO/Per-NPs) may lead to a decrease in the interaction of nanoparticles with *H. pluvilalis* and a reduction in ROS production.

Introduction

Technological developments can usually be detrimental or in the interest of a community. In addition, understanding the substances mechanism to set the necessary rules to reduce damage normally leads to the introduction of substances into the environment and the prevention of the risks to humans and the environment (Seaton et al. 2009). Several cleaning and removing methods are available for heavy metals such as ion exchange, filter membrane technology, and the other methods, which are expensive and sometimes ineffective, especially when there is heavy metal contamination of more than 100 milligrams in liters. The adsorption of heavy metals with adsorbents is one of the best methods for their removal and one of the most economical and efficient methods that can be conducted by diatomite and perlite (Shabani et al. 2017).

Algae, as food creators and valuable organisms in aquatic ecosystems, can be used as bioindicators in the rivers and freshwater lakes (Bellinger and Sigee 2015). In most cases, the entry of nanoparticles in aqueous media has negative effects on green microalgae, including the effect of graphene oxide on green algae *Raphidocelis subcapitala* and *Euglena gracilis* (Nogueira et al. 2015; Hu et al. 2015). Other studies have demonstrated the toxic effects of chromium oxide, PtNPs, AgNPs, and iron-containing nanomaterials on the growth rate, production of active oxygen species, and the activity of photosystem II in green alga *Chlamydomonas* sp. and *Chlorella* sp. (Costa et al. 2016; Sørensen et al. 2016; Nguyen et al. 2018; Lei et al. 2016; Tayemeh et al. 2020). Also, the toxic effects of other nanoparticles such as SiO_2, TiO_2, Plastic Nanoparticles, CoNPs, NiONPs, and ZnO/TiO_2-conjugated carbon-based nanohybrids on microalgae, including *Dunaliella tertiolecta*, *Pseudokirchneriella subcapitata*, *Platymonas subcordiforus*, *Chaetoceros curvisetus*, *Skeletonema costatum*, and *Thalassiosira pseudonana* have been demonstrated (Manzo et al. 2015; Morelli et al. 2018; Nolte et al. 2017;

Chen et al. 2018; Sousa et al. 2018; Wang et al. 2019; Baek et al. 2020). Further, another study has evaluated the effects of the oxides of nanoparticles on algae *Microcystis aeruginosa*, the results of which indicate that folic acid can significantly increase the toxicity of the copper oxide. Furthermore, CuO is considered as the main form of covalent nanoparticles, which may be reduced to Cu_2O in the cell. Flow-cytometric data indicate that this nanoparticle is not harmful to microalgae species (Wang et al. 2011).

Green algae *H. pluvialis* is a unicellular alga of freshwater, which is a species of Chlorophyta from the family Haematococcaceae. Haematococcus is found in many freshwater habitats in the world (Czygan 1970) and has four cycles including macrozooids, microzooids, palmella, and hematocysts. The steps of macrozooids, microzooids, and palmella are usually called the vegetative phase and the stage of hematocysts is a staggering red and stagnant phase of astaxanthin production which is called encysted (Shah et al. 2016). This green alga produces the best natural astaxanthin that is extensively applied for many foods, pharmaceuticals, and industrial uses (Lorenz 1999). Astaxanthin is synthesized in algae under cellular stress conditions and accumulates in lipid droplets (Solovchenko 2015). From a biochemical point of view, astaxanthin is synthesized from the synthetic pathway of carotenoids from glyceraldehyde-3-phosphate and pyruvate. Both of these compounds are photosynthetic products or glycolysis that enter the non-mevalonate pathway, namely, the MEP pathway, and pave the way for the production of an intermediate IPP for the synthesis of all carotenoids including astaxanthin (Miki 1991; Borowitzka 2013; Thomas and Kim 2013).

In terrestrial ecosystems, volatile organic compounds (VOCs) are widely known as an important group of infochemicals (Fink 2007). Also, VOCs from the algae can play an important role in ecosystems. This might indicate that those VOCs can transfer the stress signal between microalgae to protect against reactive oxygen species damage resulted from stress (Zuo et al. 2012). Plant polyphenolic compounds are derived from the secondary metabolism of plants (Parr and Bolwell 2000) and microalgae so that "*H. pluvialis*" can release phenolic compounds (Safafar et al. 2015).

There are several methods to prepare nanomaterials including nanoparticles, nanocomposites, nanotubes, and nanorods. These methods can be classified into three basic synthesis types: physical, chemical, and biochemical methods (Rezaei et al. 2019). Several disadvantages exist in prevalent chemical and physical approaches. Considerable environmental risks are the main drawback of these approaches due to their hazardous nature. For instance, various types of stabilizing agents, surfactants, and organic solvents are used in these techniques. In recent years, significant attention has been attracted to biochemical methods, which are named biosynthesis. In this technique, the stabilizing agents possess a biological source such as plants, alga, and so on (Ebadollahi et al. 2019). Up to now, it has been claimed that biosynthesized nanomaterials have not any considerable negative effects such as toxicity and other risks on the environment. It should be noted that the toxicity of chemically and/or physically synthesized nanomaterials on plants and alga is demonstrated (Wang et al. 2011). However, based on our knowledge, there are not any basic investigation about the toxicity of these types of nanomaterials on algae. Algae as essential components of aquatic ecosystems may be an important representative for evaluating the potential risks of biosynthesized nanomaterials on the environment. Perlites nanoparticles are one of the nanomaterials that have various applications in removing heavy metals from the water. Therefore, regarding applications of perlite in aquatic media, in this study, we investigate the effect of Per-NPs and CuO/Per-NPs on some physiological parameters of *H. pluvialis* microalgae as a case study.

Materials and methods

Preparation of the perlite nanoparticles

The chemical composition of perlite was Si, 33.8; Al, 7.2; Na, 3.4; K, 3.5; Fe, 0.6; Ca, 0.6; Mg, 0.2; trace elements, 0.2; O_2, 47.5 and H_2O, 3.0 (w/w %). Its physicomechanical properties were a white globular shape, pH 7, not soluble in water, specific area 5.3 $m^2.g^{-1}$, melting point 1200 °C, and density 3 $g.cm^{-3}$. This commercial powder was used as the starting materials. Perlite powder was first broken down to nano-size using the ball-milling technique at the frequency of 45 Hz for 20 h under the dry grinding mode (Rezaei et al. 2019; Ebadollahi et al. 2019).

Preparation of extract

The aerial parts of *all three H. pluvialis, S. angustifolium, and* walnut leaves were washed and kept in shade to dry for 72 h at 25 °C. Then they were powdered and weighted carefully. An effective method was used to extract the important metabolites; in the first step, about 10 g of the powder was shaken with 100 ml deionized water (dw) for 24 h at 25 °C. In the second step, the mixture was placed in an ultrasound bath under reduced pressure for 15 h at 25 °C. Finally, in the third step, it was placed under a radiation microwave for 5 min at 900 w and it was stored in the refrigerator (4 °C) for further experiments.

Biosynthesis CuO/Per-NPs

Based on our previously published literature, a combined method was performed to synthesize CuO/Per-NPs using all

three extracts (Jafarirad et al. 2017; 2019; 2020). Nine ml of 0.03 M CuCl$_2$ solution was added to the dispersion containing 0.4 g of perlite and 40 ml of the extract under constant stirring for 3 h at 22 °C. Subsequently, the pH of the mixture was adjusted to 7 with 1 M NaOH and refluxed for about 12 h at 100 °C. After washing with deionized water and ethanol several times, the resulting precipitate was subjected to oven drying for 1 h at 70 °C, followed by heating for 4.5 h at 390 °C.

Characterization of the as-synthesized nanoparticles

Crystalline structure and grain size were identified by XRD (D500, Siemens Diffractometer-Germany) Cu-K$_a$ radiations ($\lambda = 1.54$ Å) in 2θ range from 10° to 80°. FTIR spectra were measured by TENSOR 27–Brucker Spectrometer in the 400–4000 cm^{-1} region. The size and shape of nanomaterials were characterized using SEM and EDX techniques via MIRA3 FEG-SEM. DLS (Nanotrac Wave, Microtrac Co. USA) was used to measure the hydrodynamic diameter, size distribution, and zeta potential of samples. Deionized water was used as dispersant and pH adjusted on pH 5.7 and scattering angle of 90j was used for DLS evaluations at k = 632.8 nm. Before measurement, the samples were ultra-sonicated in a sonication bath (Bandelin Sononrex Digitec, 40KHz) was set to 25 °C for 20 min and the samples were left for 60 min before measurements.

Cultivation and treatment of algae

H. pluvialis algae were cultivated in sterile BG11 culture media (Rippka et al. 1979). Appropriate culture conditions include 25 °C and 4000-lux light intensity. Concentrations of 25–50–100 mg/L of nano-perlite were added to algal culture media at the algae exponential growth time. The mentioned concentrations were selected based on the review of articles about the various nanoparticle effects on microalga. Moreover, the number of cells was counted using a neobar lam under an optic microscope to study the small amount of alga growth at different concentrations of treatment with nano-perlite.

Photosynthetic assay

Additionally, chlorophyll *a* fluorescence was measured to evaluate the effect of nanoparticles on photosynthetic reactions. Two important indexes of chlorophyll *a* fluorescence including qY (Maximum efficiency of photosystem II) and qP (Photochemical quenching) were calculated after 24, 48, and 72 hours of treatment with nano-perlite and CuO/perlite nanoparticles at concentrations of 25, 50, and 100 mg/L (Aqua pen 100, Czech Republic).

Photosynthetic pigments

The levels of chlorophyll *a*, *b*, and the carotenoids were estimated for better evaluation of photosynthesis and conditions of nano-perlite treatment. To this end, the algae were initially centrifuged at 10,000 rpm for 10 minutes (MPW-352-Poland). Then, 80% acetone (Merk-Germany) was added to 5 mg algae biomass and it was kept at 4 °C for 24 h in the dark. The extracted pigments were measured by spectrophotometer at 470 nm, 663 nm, and 646 nm. Using the following formula, the number of pigments was calculated as well (Wellburn 1994).

$$\text{Chlorophyll a} = 12.21 \times 663 - 2.81 \times A646$$
$$\text{Chlorophyll b} = 20.13 \times A646 - 5.03 \times A663$$
$$\text{Carotene} = c_{a+b} = \frac{(100A470 - 3.27chla - 104chlb)}{198}$$

Measurement of MDA

Algae were centrifuged at 10,000 rpm for 5 minutes after 7 days of treatment. Then, it was completely powdered in liquid nitrogen, 0.5 mg of algae was suspended in 1 ml of 0.1% TCA (Merk-Germany). Then, it was centrifuged at 10,000 rpm for 5 minutes and 1 volume of the supernatant and 4 volumes of the 20% TCA were added to 0.5% TBA (Merk-Germany). The specimens were then incubated for 30 min at 95 °C in a hot water bath. Next, the absorbance of the samples was measured at 532 nm by a spectrophotometer (Boominathan and Doran 2002). Eventually, 1,1,3,3-tetraethoxypropane (Sigma-Aldrich-America) was used as the standard to calculate the amount of MDA in the fresh weight of the algae.

Measuring the amount of astaxanthin

Algae were centrifuged after reaching the final growth stage at 10,000 rpm at 25 °C and 0.01 g of alga biomass, along with 30% methanol and 5% potassium hydroxide was incubated at 95 °C for 20 min. Then, astaxanthin was extracted using DMSO (MERK-Germany) solvent (Dong et al. 2007). This pigment was measured using high-performance liquid chromatography (KNAUER, Germany) equipped with a UV detector and a reversed-phase C$_{18}$ column. The UV detector wavelength was set at 475 nm and the acetonitrile (Merck, Germany, HPLC grade) and water (3:97; Merck, Germany, HPLC grade) were used as the mobile phase in an isocratic elution program with a flow rate of 0.5 ml.min^{-1} for 5 min. Finally, the standard astaxanthin (Sigma, American) was applied to determine the peaks.

Volatile compounds assay

The sample was transferred into a vial and then the tapered end of the homemade extraction vessel was passed through the septum and inserted in the headspace of the solution. Next, 2.5 μl *n*-octanol was added to widen the section of the extraction vessel and the vial was placed at 35 °C. After 8 min, the vessel was disconnected and 1 μl of the organic phase within the narrow section of the vessel was removed using a 1-μl microsyringe and injected into the separation system.

The selected analytes were analyzed by injecting the extractant into Agilent 6890 N gas chromatograph (Agilent Technologies, CA, USA) coupled with a 5973 mass-selective detector and equipped with a split/splitless injector operated in a splitless/split mode (sampling time, 0.5 min). Then, helium (99.9999 %, Gulf Cryo, United Arabic Emirates) was used as the carrier gas at a constant flow rate of 1.0 ml min^{-1}. Chromatographic separation was achieved on an HP–5 capillary column (5% phenyl methyl siloxane, 95% dimethylsiloxane, 30 m × 0.25 mm ID, and a film thickness of 0.25 μm; Hewlett-Packard, Santa Clara, USA) with an initial temperature of 50 °C (held 5 minutes), ramped at 8 °C min^{-1} to 300 °C, and held at 300 °C for 5 minutes. MS operational conditions included an electron ionization at 70 eV, an ionic source temperature of 250 °C, a transfer line temperature of 260 °C, the mass range of m/z 55–350, an acquisition rate of 20 Hz, and a detector voltage of –1700 V. Library searching was performed using the commercial NIST library.

Statistical survey

In this research, treatments were performed applying a complete randomized design (One-way ANOVA) with four treatments. Statistical analysis of the data was conducted using SPSS 24 and the charts were plotted using Excel 2016 software. The means were compared with Duncan's multiple range test ($P \leq 0.05$).

Results and discussion

Structural features of as-synthesized nanomaterials were analyzed using XRD, FESEM, EDX, TEM, and FTIR techniques.

Structural characterization of CuO/Per-NPs

XRD diffractograms

XRD diffractograms of Per-NPs and CuO/Per-NPs showed significant differences as shown in Fig. 1A-D. Per-NPs
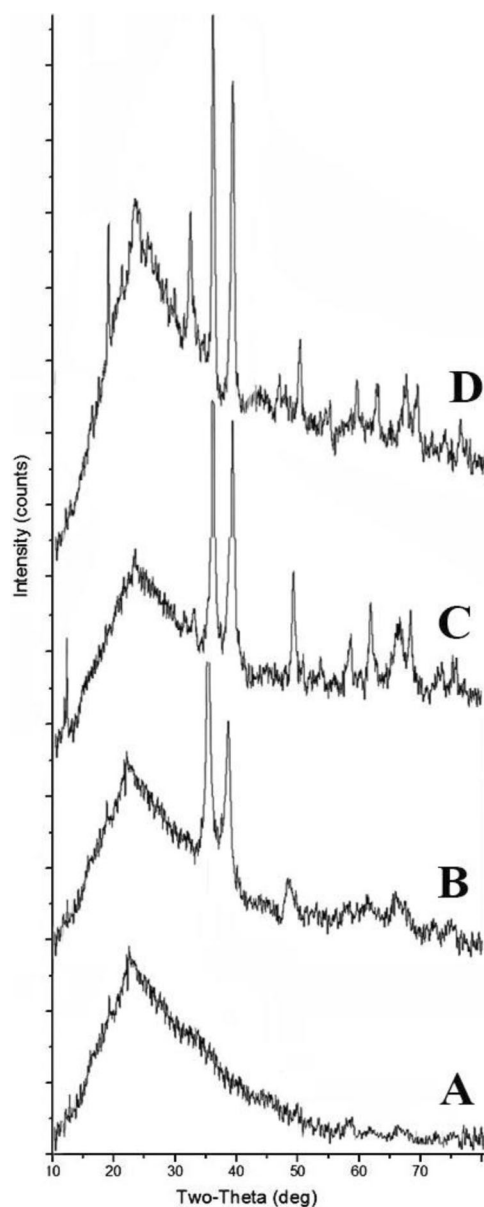

Fig. 1 XRD diffractograms of (**A**) Per-NPs, (**B**–**D**) the as-synthesized CuO/Per-NPs using the extract of *H. pluvialis, S. angustifolium, and* walnut leaves, respectively

represented a characteristic peak at 2θ around 25.53. This well-defined broad reflection has an amorphous entity (Rezaei et al. 2019; Ebadollahi et al. 2019). The peak positions with 2θ value of 32.79°, 35.45°, 38.21°, 48.13°, 53.56°, 58.95°, 61.14°, 66.12°, 69.51, 74.39 and 77.98° are indexed as to the [110], [002], [111], [202], [020], [202], [113], [311], [220], [311] and [004] planes, respectively. These peaks were observed in the XRD diffractograms of all CuO/Per-NPs when CuO was immobilized on the surface of perlite (Fig. 1B-D). All peaks of CuO were matched according to ICDD data (card No. 410254) using all three extracts (Rasoulpour and Jafarirad 2017).
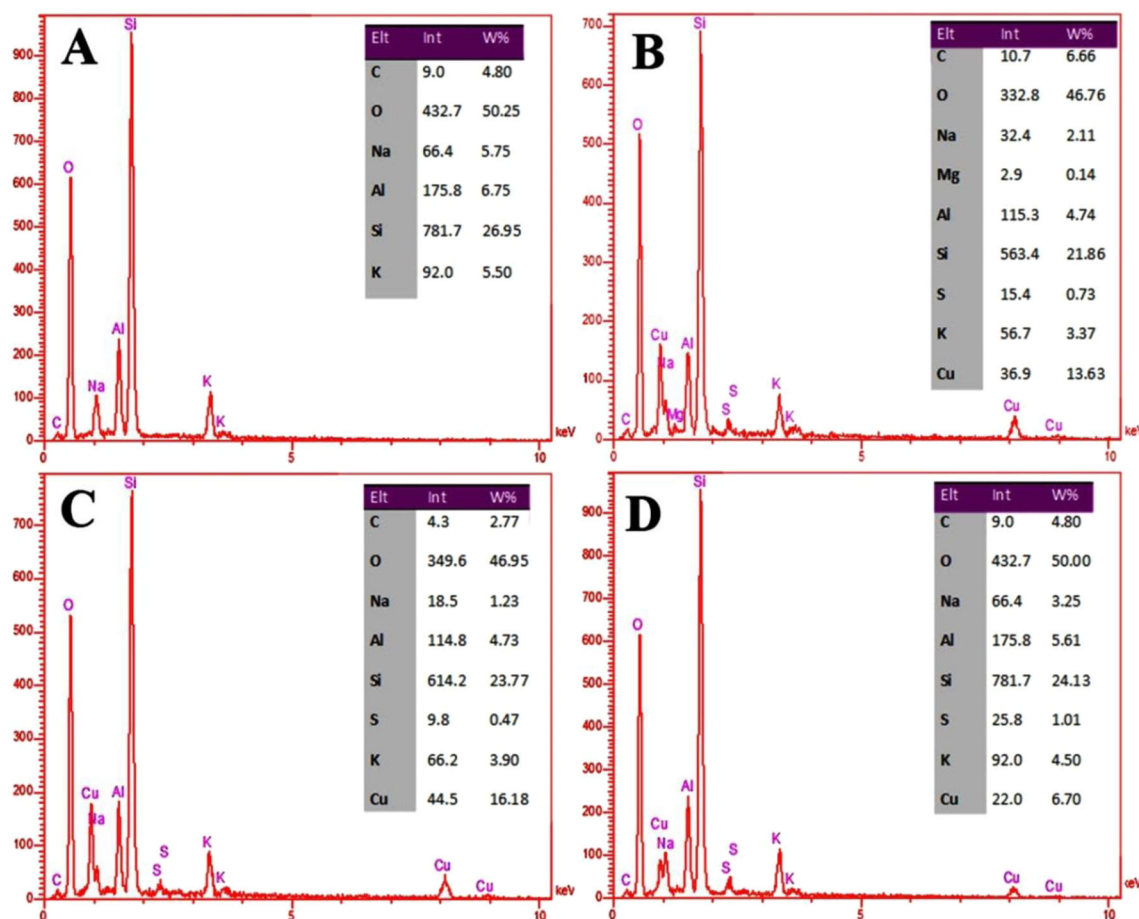
Fig. 2 A EDX diffractograms of (**A**) Per-NPs, (**B–D**) the as-synthesized CuO/Per-NPs using the extract of *H. pluvialis, S. angustifolium, and* walnut leaves, respectively

EDX pattern

The EDX results of the Per-NPs and CuO/Per-NPs were shown in Fig. 2A-D. The presence of K, Al, Si, and oxygen elements of the perlite can be proved by EDX analysis. As Fig. 2B-D show, the presence of Cu element in the EDX spectra indicates the immobilization of Cu on the perlite. Using an extract of *H. pluvialis, S. angustifolium, and* walnut leaves, the weight percentage of Cu was found to be 13.63, 16.18, and 6.70% (w/w) respectively. Moreover, EDX spectra show the signal of carbon element attached to the CuO/Per-NPs due to phytochemicals in the extract.

Morphological and colloidal studies

The FESEM images of as-synthesized samples were illustrated in Fig. 3B-D. The FESEM micrograph of perlite (Fig. 3A) reveals the sheet-like morphology of perlite as good support. The FESEM micrographs of CuO/Per-NPs (Fig. 3B-D) show that these NPs are mainly globular which

were immobilized homogeneously onto the perlite sheets. The average size of the CuO nanoparticle was 13–24 nm (Fig. 3B-D). The activity of the as-synthesized NPs depends on the particle size (Jafarirad et al. 2018).

During this study, the size, size distribution, and surface charge of dispersed NCs were monitored by DLS. Since DLS measure the hydrodynamic diameter, the value of size obtained by this technique, owing to the entity of DLS, can be larger than the value obtained by using FESEM. The DLS diagrams of as-synthesized samples were illustrated in Fig. 4B-D. The DLS diagram of perlite (Fig. 4A) indicates that the diameter was 35.3 nm. Hence, from Fig. 4A, it can prove that the perlite used in this study has a nano-scale range. Besides, the polydispersity index (PDI) is 0.62 (Table 1). Figure 4B-D show the size of as-synthesized CuO/Per-NPs. According to our findings, the amount of zeta potential for colloidal suspensions of as-synthesized CuO/Per-NPs was found between +20–25 mV (Table 1). Since the high absolute zeta potential value exerts a strong repulsive force among the CuO/Per-NPs, these data for zeta potential are acceptable in accordance with DLVO theory.
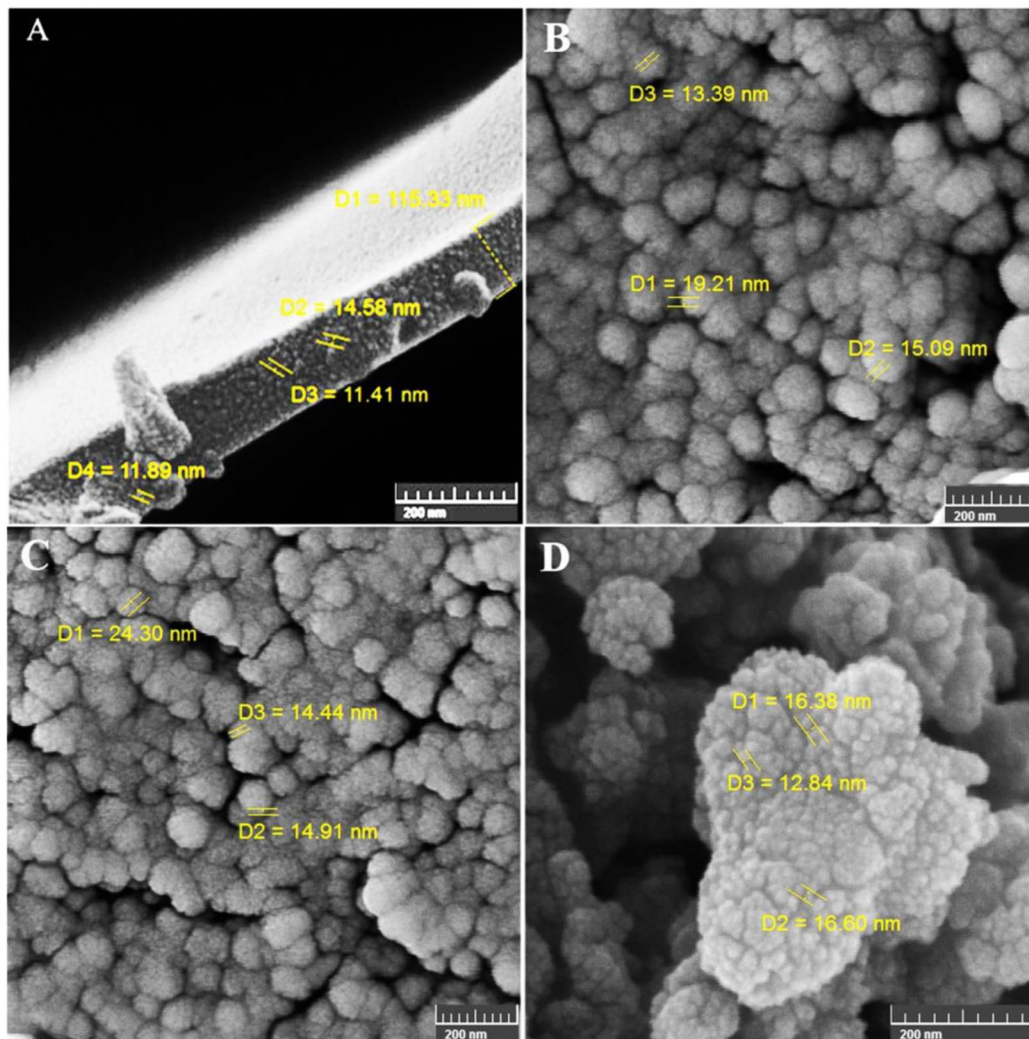
Fig. 3 FESEM images of (**A**) Per-NPs, (**B–D**) the as-synthesized CuO/Per-NPs using extract of *H. pluvialis, S. angustifolium, and* walnut leaves, respectively

FTIR characterization

The as-synthesized CuO/Per-NPs are bio-capped by the phytochemicals of *H. pluvialis, S. angustifolium, and* walnut leaves in the extract. This is due to the presence of phytochemicals in all extracts such as Flavonoids, Carbohydrates, Alkaloids, and Phenolic compounds (Jafarirad et al. 2018). The FT-IR spectra of Per-NPs and CuO/Per-NPs can be seen in Fig. 5A-D. In these figures, the bonds at 458 and 791 cm^{-1} corresponded to Al-O and Si-O stretching vibration bond, respectively. These peaks are the main features in perlite and other aluminosilicate phases (Rezaei et al. 2019). The peak on 672 cm^{-1} was assigned to the Cu-O stretching bands. Moreover, the prominent peaks at 3609, 3740, and 3847 cm^{-1} are related to water-bound directly to Si-O-H, Cu-O-H, and Al-O-H, respectively (Ebadollahi et al. 2019).

Besides, the bonds at 2922, 1530, and 1698 cm^{-1} corresponded to aliphatic (C-H), olefin (C=C), and carbonyl (C=O) stretching vibration bond, respectively. These peaks are the main features of phytochemical metabolites of all three extracts (Jafarirad et al. 2018).

Evaluation of H. pluvialis growth

After the treatment of algae with nano-perlite, it was determined that this nanoparticle had a negative effect on the growth of alga at different concentrations (i.e., 25, 50, and 100 mg/L) during three days, and the growth of algae decreased significantly in all treated concentrations. Full growth was observed in the control sample, but a significant decrease was observed at the concentrations of 50 mg/L and 100 mg/L Per/NPs. Growth changes were significantly

Fig. 4 DLS patterns of the (**A**) Per-NPs, (**B–D**) the as-synthesized CuO/Per-NPs using an extract of *H. pluvialis, S. angustifolium, and* walnut leaves, respectively
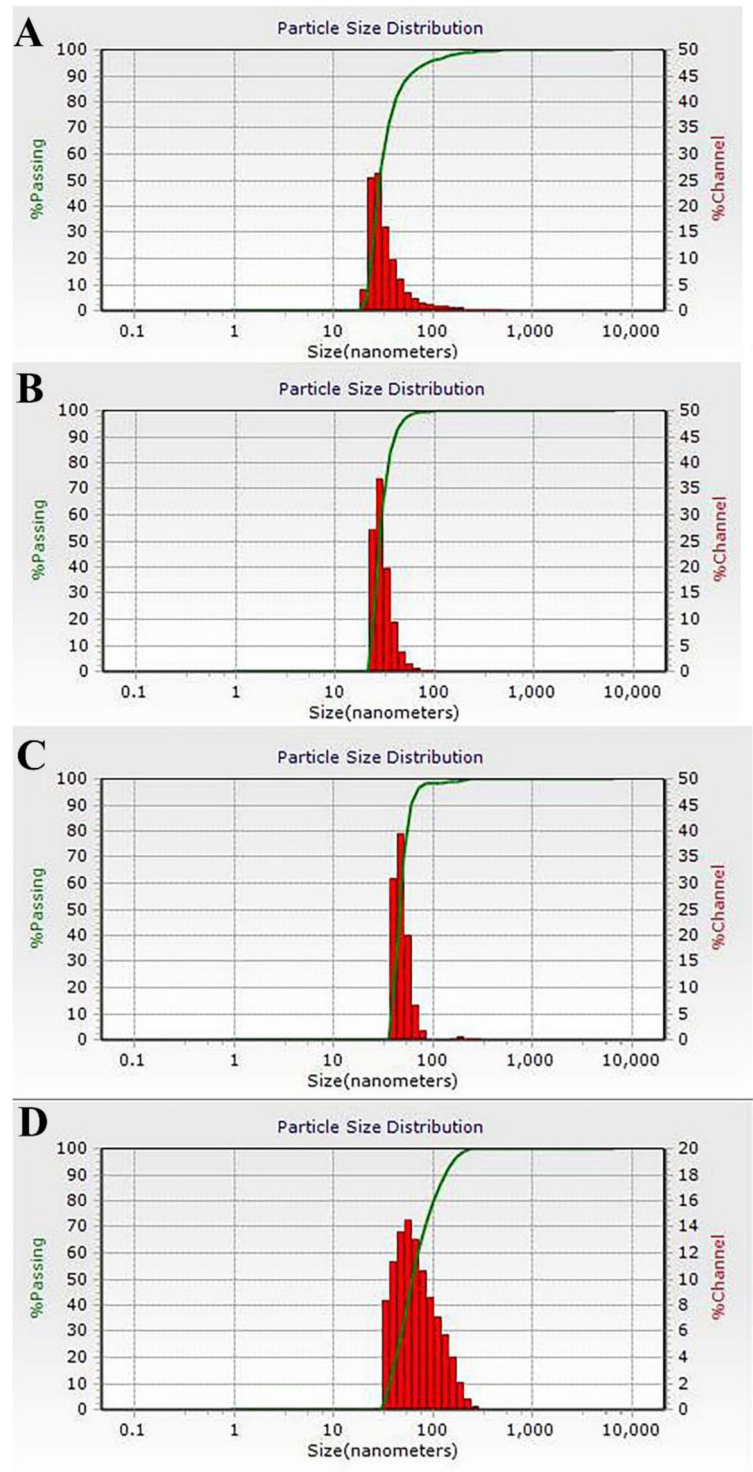
different at concentrations of 25, 50, and 100 mg/L, simultaneously with the increase in the number of treatment days.

The nanoparticles properties results showed that there was no difference in the nanoparticles synthesized by all three extracts, so the nanoparticles synthesized by the *H. pluvialis* algae extract was used for subsequent experiments. To make

sure, the experiments were repeated with *S. angustifolium* algae and walnut leaves, and the results were the same. Therefore, in experiments to investigate the effect of modified nanoperlites, synthesized CuO/perlite nanoparticles using *H. pluvialis* extract were used. The maximum growth rate of algae was observed 72 h after treatment with 25 mg/L of CuO/perlite nanoparticles, but there was no significant

Table 1 Colloidal properties of the (A) Per-NPs, (B–D) the as-synthesized CuO/Per-NPs using an extract of *H. pluvialis*, *S. angustifolium, and* walnut leaves, respectively

Samples	D(nm)		PDI (μ_2/T^2)[c]	Z[d] (mV)
	SEM[a]	DLS[b]		
A	11–14	35.30	0.62	+16.72
B	13–19	37.97	0.43	+24.23
C	12–24	68.51	0.22	+23.44
D	12–16	71.23	0.87	+22.89

[a]Particle mean diameter measured by SEM

[b]Hydrodynamic diameter measured by DLS in water

[c]Polydispersity index based on DLS

[d]zeta potential

difference between the growth rate of algae in control conditions and treatment with 100 mg/L CuO/perlite (Fig. 6).

Photosynthetic assay

Chlorophyll *a* fluorescence assay was evaluated to investigate the effect of nanoparticles on photosynthetic reactions. Two important indices of chlorophyll *a* fluorescence were investigated in this respect. The maximum efficiency of the photosystem II (qY) showed a significant reduction between the control and the three levels of perlite nanoparticles in terms of the qY index after 24, 48, and 72 h. The photochemical quenching (qP) is applied as an indicator to show the extent of photosystem II reaction centers that are open so that the saturation of photosynthesis and the electron transport chain by light can cause a change in this index. The qP index represented a significant decrease after 24 h of treatment with a concentration of 50 and 100 mg/L nanoperlites compared to the control and 25 mg/L nano-perlite. Besides, a reduction was observed in qP after 48 and 72 h of treatment with concentrations of 50 and 100 mg per liter (Table 2).

The qY parameter was unchanged at concentrations of 25, 50, and 100 mg/L of CuO/perlite nanoparticles, 24, 48 and 72 h after treatment with CuO/perlite nanoparticles. The qP parameter was increased slightly at 100 mg/L of CuO/perlite after 48 h of treatment.

The fluorescence indicators of chlorophyll *a* are used to study the photochemical reactions in photosystem II and the components of the electron transport chain (Maxwell and Johnson 2000). The results of this study indicated that the treatment of *H. pluvialis* with different concentrations of Per-NPs decreased the yield of maximum efficiency of the photosystem II, as well as it was effective on the rate of open PSII reaction centers. Several studies demonstrated that the qY index is relatively stable against various stresses and only decreases in the conditions of severe damage to

photosystem II while the qP index is more sensitive and changes with different stresses (Maxwell and Johnson 2000; Solovchenko et al. 2013; Le Faucheur et al. 2005).

Since the qY and qP indexs did not show much difference after treatment with different concentrations of Cuo/ perlite nanoparticles, it can be concluded that these nanoparticles do not cause serious damage to the photosynthetic apparatus that is associated with growth rate results.

Photosynthetic pigments

The photosynthetic pigmentation of chlorophyll *a* increased after 3 days of culturing in 25 mg/L treatments of nanoperlite compared to the control. The increase of chlorophyll *a* at the concentrations of 50 mg/L and 100 mg/L also showed a significant increase compared to the control. Further, the maximum increase of chlorophyll *a* pigmentation was observed at 25 mg/L concentration of nanoperlites. However, a slight increase was found in 50 mg/L compared to 25 mg/L of nano-perlite, but this pigment increased again at a 100 mg/L concentration. Furthermore, chlorophyll *b* content demonstrated a significant increase at different concentrations of the treatment compared to the control (Similar to chlorophyll *a*). The maximum increase was recorded at 25 mg/L concentration of nano-perliltes. Moreover, the increase of chlorophyll *a* to chlorophyll *b* ratios was detected at a concentration of 100 mg/L. Conversely, carotenoid pigments represented a significant increase at different concentrations of 25 and 100 mg/L similarity.

The photosynthetic pigments of chlorophyll *a* and *b* increased in response to nano-perlite stress compared with the control sample. An increase in the concentration of the pigments is due to the increased ability of microalgae for light absorbing. According to research regarding nanoparticle effects on microalgae, it is confirmed that the increased chlorophyll concentration at toxic concentrations of nanoparticles increases the concentration of chlorophylls, as well as the ratio of chlorophyll *a* to chlorophyll *b*, which increases the absorption of light by the algae (Wang et al. 2010). Increasing the ratio of chlorophyll *a* to chlorophyll *b* could also be due to the production of free oxygen radicals within the microalgae due to the effect of nanoparticles (Chen et al. 2012). Total carotenoids increase in response to nano-perlite treatment, which confirms the stress condition for *H. pluvialis* in the presence of nano-perlite. Previous research documented the enhancement of carotenoids in titanium dioxide nanoparticles on green microalgae (Chen et al. 2012).

About CuO/perlite nanoparticles effect, the change of chlorophyll *a* amount was equal between 50 mg/L CuO/ perlite nanoparticles and control condition after 3 days of treatment and increased at 25 and 100 mg/L concentrations. The amount of chlorophyll *b* in the control culture and different concentrations of CuO/perlite did not show

Fig. 5 FTIR patterns of the of
(**A**) Per-NPs, (**B–D**) the as-
synthesized CuO/Per-NPs using
the extract of *H. pluvialis, S.
angustifolium*, and walnut
leaves, respectively
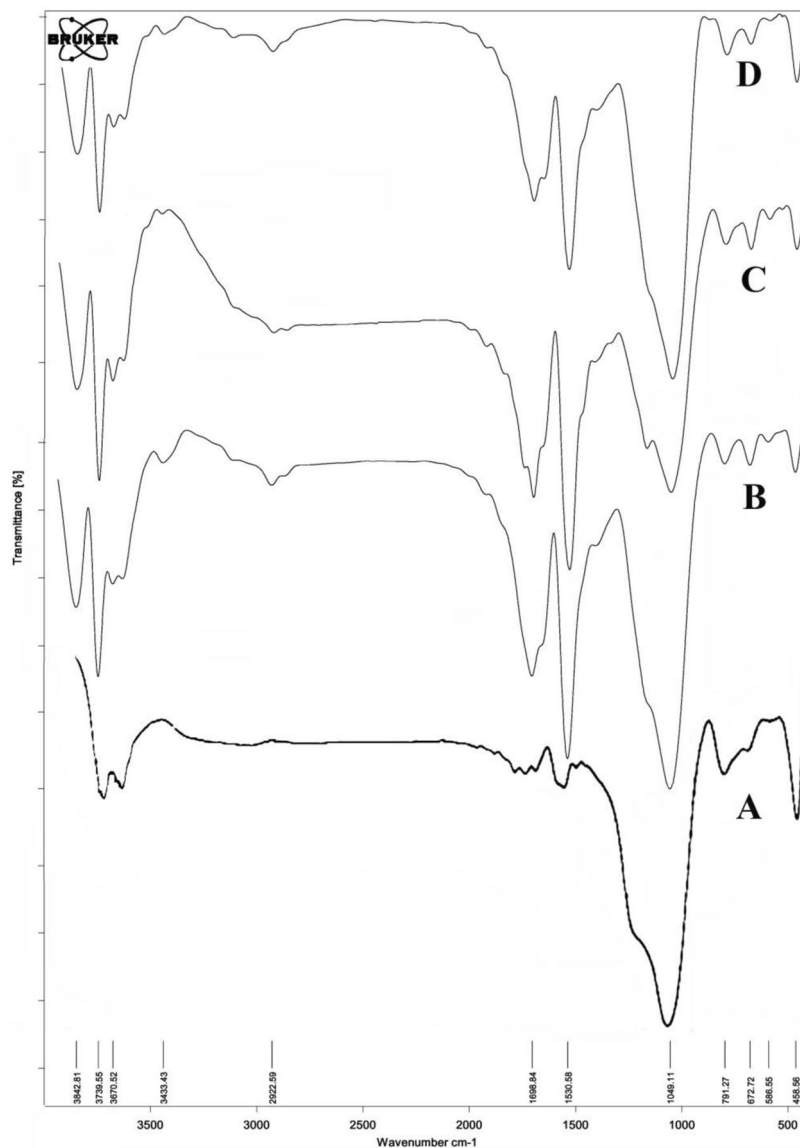
significant changes. The concentration of carotenoid pigments in the concentrations of 25 and 100 mg/L were equal and showed a significant increase. (Table S1). In general, the changes in the studied pigments after treatment with nanoperlite are more severe than the treatment with CuO/perlite nanoparticles.

Malondialdehyde (MDA) assay

MDA assay was performed to investigate the effect of nanoparticles on the integrity of alga membranes. According to the obtained results for perlite nanoparticles, an increased concentration of MDA was assayed after 25, 50, and 100 mg/L treatment compared to the control (Fig. 7A). An increase in MDA content is consistent with a decrease in the growth rate.

Three days after treatment, the amount of MDA in the control culture and different concentrations of CuO/perlite was not different, that is, the growth stimulation was performed by the membrane protection by CuO/perlite nanoparticles. This result, together with the results related to the growth rate shows non-toxicity or low toxicity of CuO/perlite compared to perlite nanoparticles. Also, based on Pearson Correlation analysis, there is a negative and significant correlation between growth rate and MDA content (Table 3).

The concentration of MDA is in its maximum value at concentration of 50 and 100 mg/L perlite nanoparticles, which indicates that the stress is responsible for the membrane integrity. The tension produces free radicals of oxygen in the cells. These free oxygen radicals cause the peroxidation of the membranes and thus leads to the production of MDA. However, the concentration of MDA increases, which

Fig. 6 The growth rate of *H. pluvialis* after treatment with different concentrations of perlite (Per/NPs) and CuO/perlite nanoparticle (mg/L) with three replicates for three days. Values marked with the same letters do not differ significantly ($P \leq 0.05$). Vertical bars mean SD
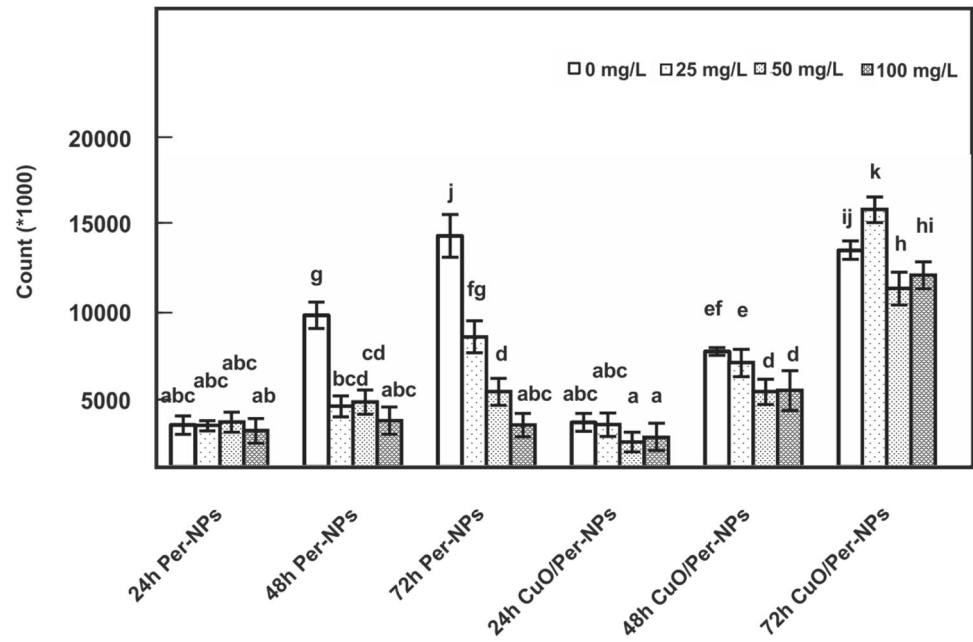

Table 2 Chlorophyll *a* Fluorescence parameters in *H. pluvialis* grown in liquid culture for one week and treated with different concentrations of perlite and CuO/perlite nanoparticles in three different time intervals. Means ± SD in columns marked with the same letters do not differ significantly ($P \leq 0.05$)

Per-NPs (mg/L)	qY		
	24 h	48 h	72 h
0	0.78 ± 0.00^b	0.79 ± 0.00^b	0.79 ± 0.01^b
25	0.61 ± 0.19^a	0.75 ± 0.01^b	0.75 ± 0.01^b
50	0.69 ± 0.01^{ab}	0.72 ± 0.02^b	0.73 ± 0.00^b
100	0.71 ± 0.02^{ab}	0.70 ± 0.01^{ab}	0.69 ± 0.00^{ab}
	qP		
0	0.81 ± 0.01^{de}	0.81 ± 0.03^{de}	0.80 ± 0.01^{cde}
25	0.82 ± 0.02^e	0.81 ± 0.01^{de}	0.79 ± 0.02^{cde}
50	0.74 ± 0.01^{ab}	0.77 ± 0.01^{bcd}	0.76 ± 0.01^{bcd}
100	0.72 ± 0.00^a	0.76 ± 0.03^{abc}	0.76 ± 0.00^{abc}

CuO/Per-NPs (mg/L)	qY		
	24 h	48 h	72 h
0	0.78 ± 0.03^a	0.79 ± 0.00^a	0.80 ± 0.04^a
25	0.79 ± 0.00^a	0.78 ± 0.01^a	0.78 ± 0.01^a
50	0.80 ± 0.06^a	0.78 ± 0.02^a	0.79 ± 0.02^a
100	0.80 ± 0.05^a	0.80 ± 0.03^a	0.80 ± 0.00^a
	qP		
0	0.80 ± 0.04^{ab}	0.79 ± 0.04^{ab}	0.78 ± 0.01^{ab}
25	0.79 ± 0.01^{ab}	0.79 ± 0.01^{ab}	0.76 ± 0.00^a
50	0.79 ± 0.01^{ab}	0.80 ± 0.01^{ab}	0.79 ± 0.01^{ab}
100	0.78 ± 0.00^{ab}	0.81 ± 0.01^b	0.80 ± 0.03^{ab}

indicates the extent of membrane degradation. Reducing MDA levels can be due to the increased activity of antioxidant enzymes, but the concentration of MDA release varies in different lifetimes of the plants and algae (Savicka and Škute 2010).

Analysis of astaxanthin

To assay, the effect of nano-perlite on the astaxanthin production in *H. pluvialis*, the standard astaxanthin (Sigma, Germany) at concentrations of 10, 7.5, 5, 2.5, 1, and 0.5 mg/mL was used to draw the standard curve. Based on the result, the concentrations of astaxanthin decreased in most perlite and CuO/perlite nanoparticles treatments in comparison with the control. Besides, the rate of decrease in astaxanthin content in the presence of different concentrations of Per-NPs was higher than the rate of decrease in the presence of different concentrations of CuO/Per-NPs (Fig. 7B). Despite an increase in total carotenoids in the presence of most concentrations used for Per-NPs and CuO/Per-NPs, the amount of astaxanthin has decreased, indicating that the share of other types of carotenoids in the presence of nanoperlites and their modified derivatives has increased. However, the amount of produced astaxanthin in the presence of modified nanoperlite (CuO/perlite nanoparticles) is higher than that of nanoperlite.

Reducing the amount of astaxanthin in treated samples can be due to the rapid loss of algae growth due to the high toxicity of nanoparticles, that correlation analysis shows positive and significant correlation between growth rate and

Fig. 7 A MDA concentration in *H. pluvialis* algae grown in the liquid culture for one week and then treated with four different replicates with different concentrations of perlite and CuO/perlite nanoparticles (mg/L) for three days. **B** Astaxanthin content in algae treated with perlite and CuO/perlite nanoparticles measured one week after treatment with four different replicates. Values marked with the same letters do not differ significantly ($P \leq 0.05$). Vertical bars mean SD
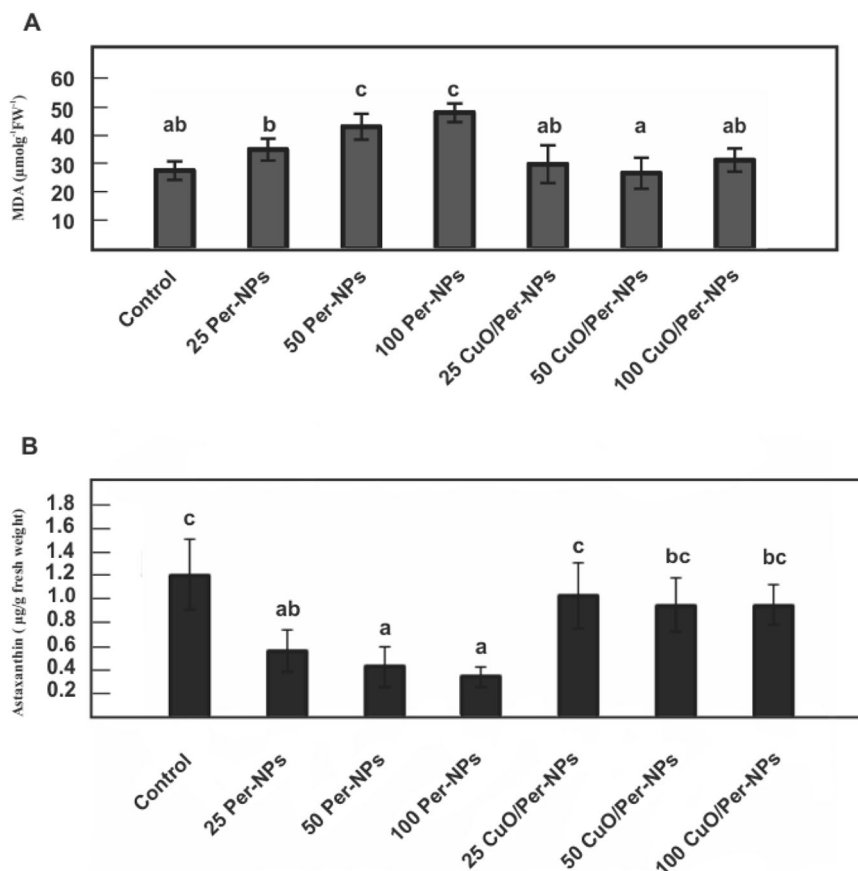

Table 3 The results of Pearson correlation analysis

	MDA	Growth	Astaxanthin	qY	qP	Chla	Chlb
Growth	−0.793[a]						
Astaxanthin	−0.788[a]	0.703[a]					
qY	−0.703[a]	0.814[a]	0.590[a]				
qP	−0.281	0.297	0.032	0.475[b]			
Chla	0.500[b]	−0.459[b]	−0.593[a]	−0.453[b]	−0.028		
Chlb	0.449[b]	−0.607[a]	−0.564[a]	−0.571[a]	−0.025	0.883[a]	
carotenoid	0.210	−0.146	−0.348	−0.318	−0.231	0.609[a]	0.477[b]

[a]Correlation is significant at the 0.01 level (two-tailed)

[b]Correlation is significant at the 0.05 level (two-tailed)

astaxanthin concentration. Based on the report of another study on astaxanthin biosynthesis and accumulation, astaxanthin concentration may be low at a time of decreasing growth and there is a direct relationship between the amount of biomass and astaxanthin.

The results of the present study show that CuO/perlite nanoparticles in addition to a positive role in the growth rate of algae do not have a negative effect on the production of astaxanthin. For commercial purposes, the use of this compound can be considered in astaxanthin production. Nanoperlite, due to the reduction of algae biomass and a decrease in the yield of astaxanthin production, is not a good option for this purpose.

Volatile compounds

Investigating the effect of nanoparticles on produced volatile compounds by algae can be valuable because volatile compounds can alter the taste and smell of water and make it difficult to use. Regarding the different applications of Per-NPs and their entry into water sources, the effect of Per-NPs was investigated on *H. pluvialis* volatile compounds. The volatile compounds detection showed that the detected monoterpene in the time of 4.791 in the control samples disappeared in 25, 50, and 100 mg/L treatments. Besides, at 5.587 Tartronic acid, which was recorded in the control sample, volatile compounds were changed to phenolic ones

at 25 and 50 mg/L of nano-perlite while no compound was recorded at 100 mg/L concentration. Further, glycerin (as sugar alcohol) was detected in control and treated samples except for 50 mg/L at 7.279. Furthermore, benzene compounds were observed at 8.38 only at a concentration of 100 mg/L nano-perlite. At the time of 15.610, phenolic compounds were detected in the control and treated samples. The produced phenolic compounds increased at 25 mg/L concentration compared to the control and other concentrations, but phenolic compounds decreased at the concentrations of 50 and 100 mg/L of nano-perlite compared to the control (Table S2).

Volatile organic compounds (VOCs) production by algae is a major concern in water processing since algae are the reason for regularly encountered taste and odor problems in drinking water (Fink 2007). Based on our results, nano-perlite can change the VOCs profile, but compared to the control samples these changes were negligible.

Conclusion

The present study has confirmed that CuO/Per-NPs can be successfully synthesized using aqueous extract of *H. pluvialis, S. angustifolium,* and walnut leaves. This synthesis method resulted in producing a uniform size distribution of CuO/Per-NPs around 13–24 nm. NPs have a toxic effect on unicellular algae *H. pluvialis*, which is a representative of freshwater alga. Based on the role of algae as food creators in aquatic ecosystems, this nanoparticle can have negative effects on the environment. According to the results of HPLC, the amount of astaxanthin is reduced in treated alga with this nanoparticle, rendering that it is not suitable for use in biotechnology to increase the production of this valuable pigment.

In general and based on the Pearson correlation analysis about studied parameters, there is a positive and significant correlation between growth rate and qY. While, there is a significant but negative correlation between growth rate and MDA content. The positive relationship between increasing growth rate and performance of photosynthetic reactions seems logical, which is also indicated by the results of statistical analysis. On the other hand, an increase in MDA indicates a change in membrane integrity and stress conditions, which is also confirmed by a decrease in growth rate.

Unlike the perlite nanoparticles, its modified derivative (CuO/perlite) not only did not reduce growth but also increased it. The optimal concentration of this compound was 25 mg/L. This increase was associated with no change in photochemical reactions, MDA content and the amount of astaxanthin. Therefore, the toxicity of biosynthesized CuO/Per-NPs appears to be lower than that of Per-NPs

which are used as superabsorbent of heavy metals in a water environment.

The reason for the difference in the response of algal growth to perlite nanoparticles with its modified derivative can be due to its coating with nano-copper, which has prevented its possible absorption and toxic effect of this nanoparticle. The effects of nanoparticles on living organisms and cells, along with their chemical composition and dose, are dependent on various factors such as size, surface properties, dissolution, self-assembly, quantum effects, concentration, and aggregation. Therefore, in addition to size, surface properties such as surface charge are the main factors of nanoparticles toxicity, especially metal oxide nanoparticles, and reduced toxicity of nanoparticles with metal oxide has been shown with increased cation charge. So that the change in the surface may lead to reduced interaction between nanoparticles and cells and living organisms such as microalgae, which can be explained by the electromagnetic attraction that with the decrease of surface cation charge easier accumulation between nanoparticles with living organisms from bacteria and algae can occur. The toxicity mechanisms of nanoparticles depend mainly on the interaction between nanoparticles, biomolecules, and living cells, so that different nanoparticle can pass directly through the membrane, via ion channels, carrier proteins, and endocytosis. NPs Interaction with mitochondria and redox-active proteins can stimulate ROS generation in addition to blocking the cell's antioxidant defense systems. The produced ROS causes the damage of one or two strands of DNA or point mutations and affects the expression of genes. Nanoparticles can also disrupt the signal cascade activation pathway by interacting with cellular signal molecules, DNA damage, and cell death.

According to reports, the release of metal ions from nanoparticles is minimal, and low concentrations of copper cause negligible toxic effects on living organisms, in which cell type and cell wall characteristics are of particular importance. Therefore, it seems that by changing the surface of nanoperlit (CuO/Per-NPs) and changing the cationic charge, the interaction of these nanoparticles with *H. pluvilalis* is reduced and the toxicity and production of ROS are reduced.

Also, Copper, being a micronutrient, is essential for photosynthesis, so this may be a justification for the low toxicity of modified nanoperlites (CuO/Per-NPs) compared to nanoperlites. More studies are needed in this case.

Data availability

Data are available by contacting JR (jafar_razeghi@tabrizu. ac.ir) and SJ (jafarirad@tabrizu.ac.ir)

Compliance with ethical standards

References

Baek S, Joo SH, Su C, Toborek M (2020) Toxicity of ZnO/TiO$_2$-conjugated carbon-based nanohybrids on the coastal marine alga Thalassiosira pseudonana. Environ Toxicol 35(1):87–96

Bellinger EG, Sigee DC (2015) Freshwater algae: identification and use as bioindicators. John Wiley & Sons

Boominathan R, Doran PM (2002) Ni-induced oxidative stress in roots of the Ni hyperaccumulator, Alyssum bertolonii. New phytol 156 (2):205–215

Borowitzka MA (2013) High-value products from microalgae—their development and commercialisation. J appl phycol 25 (3):743–756

Chen L, Zhou L, Liu Y, Deng S, Wu H, Wang G (2012) Toxicological effects of nanometer titanium dioxide (nano-TiO$_2$) on Chlamydomonas reinhardtii. Ecotoxicol Environ Saf 84:155–162

Chen X, Zhang C, Tan L, Wang J (2018) Toxicity of Co nanoparticles on three species of marine microalgae. Environ Pollut 236:454–461

Costa CHD, Perreault F, Oukarroum A, Melegari SP, Popovic R, Matias WG (2016) Effect of chromium oxide (III) nanoparticles on the production of reactive oxygen species and photosystem II activity in the green alga Chlamydomonas reinhardtii. Sci Total Environ 565:951–960

Czygan F (1970) Blood-rain and blood-snow: nitrogen-deficient cells of *H. pluvialis* and Chlamydomonas nivalis. Archiv fur Mikrobiologie 74(1):69–76

Dong Q, Zhao X, Xing X, Hu J, Gong JNH (2007) Secretion during astaxanthin synthesis in *H. pluvialis* under high irradiance and nitrogen defi-cient conditions. Chin J Chem Eng 15(2):162–166

Ebadollahi R, Jafarirad S, Kosari-Nasab M, Mahjouri S (2019) Effect of explant source, perlite nanoparticles and TiO 2/perlite nanocomposites on phytochemical composition of metabolites in callus cultures of Hypericum perforatum. Sci Rep 9(1):1–15

Fink P (2007) Ecological functions of volatile organic compounds in aquatic systems. Mar Freshw Behav Physiol 40(3):155–168

Jafarirad S, Kordi M, Kosari-Nasab M (2017) Extracellular one-pot synthesis of nanosilver using Hyssopus officinalis L.: a

biophysical approach on bioconstituent-Ag+ interactions. Inorg Nano-Met Chem 47:632–638

Jafarirad S, Rasoulpour I, Divband B, Hammami Torghabe I, Kosari-Nasab M (2018) Innovative biocapped CuO nano-photocatalysts: a rapid and green method for photocatalytic degradation of 4-nitrophenol. Mater Res Innov 22(7):415–421

Jafarirad S, Salmasi M, Divband B, Sarabchi M (2019) Systematic study of Nd^{3+} on structural properties of ZnO nanocomposite for biomedical applications; in-vitro biocompatibility, bioactivity, photoluminescence and antioxidant properties. J Rare Earths 37:508–514

Jafarirad S, Taghizadeh PM, Divband B (2020) Biosynthesis, characterization and structural properties of a novel kind of Ag/ZnO nanocomposites in order to increase its biocompatibility across human A549 cell line. Bionanoscience 10:42–53

Hu C, Wang Q, Zhao H, Wang L, Guo S, Li X (2015) Ecotoxicological effects of graphene oxide on the protozoan Euglena gracilis. Chemosphere 128:184–190

Le Faucheur S, Behra R, Sigg L (2005) Phytochelatin induction, cadmium accumulation, and algal sensitivity to free cadmium ion in Scenedesmus vacuolatus. Environ Toxicol Chem 24 (7):1731–1737

Lei C, Zhang L, Yang K, Zhu L, Lin D (2016) Toxicity of iron-based nanoparticles to green algae: effects of particle size, crystal phase, oxidation state and environmental aging. Environ Pollut 218:505–512

Lorenz RT (1999) A technical review of Haematococcus algae NatuRoseTM Tech Bull 60:1–12

Manzo S, Buono S, Rametta G, Miglietta M, Schiavo S, Di, Francia G (2015) The diverse toxic effect of SiO$_2$ and TiO$_2$ nanoparticles toward the marine microalgae Dunaliella tertiolecta. Environ Sci Pollut Res 22(20):15941–15951

Maxwell K, Johnson GN (2000) Chlorophyll fluorescence—a practical guide. J Exp Bot 51(345):659–668

Miki W (1991) Biological functions and activities of animal carotenoids. Pure Appl Chem 63(1):141–146

Morelli E, Gabellieri E, Bonomini A, Tognotti D, Grassi G, Corsi I (2018) TiO2 nanoparticles in seawater: aggregation and interactions with the green alga Dunaliella tertiolecta. Ecotoxicol Environ Saf 148:184–193

Nguyen NH, Von Moos NR, Slaveykova VI, Mackenzie K, Meckenstock RU, Thümmler S, Bosch J, Ševců A (2018) Biological effects of four iron-containing nanoremediation materials on the green alga Chlamydomonas sp. Ecotoxicol Environ Saf 154:36–44

Nogueira P, Nakabayashi D, Zucolotto V (2015) The effects of graphene oxide on green algae Raphidocelis subcapitata. Aquat Toxicol 166:29–35

Nolte TM, Hartmann NB, Kleijn JM, Garnæs J, Van De Meent D, Hendriks AJ, Baun A (2017) The toxicity of plastic nanoparticles to green algae as influenced by surface modification, medium hardness and cellular adsorption. Aquat Toxicol 183:11–20

Parr AJ, Bolwell GP (2000) Phenols in the plant and in man. The potential for possible nutritional enhancement of the diet by modifying the phenols content or profile. J Sci Food Agric 80 (7):985–1012

Rasoulpour I, Jafarirad S (2017) Synthesis of biocapped CuO nanoparticles: an investigation on biorganic-Cu^{2+} interactions, in vitro antioxidant and antimicrobial aspects. Inorg Nano-Met Chem 47 (11):1599–1604

Rezaei Z, Jafarirad S, Kosari-Nasab M (2019) Modulation of secondary metabolite profiles by biologically synthesized MgO/perlite nanocomposites inMelissa officinalis plant organ cultures J Hazard Mater 3800:120878–12089

Rippka R, Deruelles J, Waterbury JB, Herdman M, Stanier RY (1979) Generic assignments, strain histories and properties of pure cultures of cyanobacteria. Microbiology 111(1):1–61

Safafar H, Wagenen JV, Møller P, Jacobsen C (2015) Carotenoids, phenolic compounds and tocopherols contribute to the antioxidative properties of some microalgae species grown on industrial wastewater. Mar Drugs 13(12):7339–7356

Savicka M, Škute N (2010) Effects of high temperature on MDA content, superoxide production and growth changes in wheat seedlings (Triticum aestivum L.). Ekologija 56(1):26–33

Seaton A, Tran L, Aitken R, Donaldson K (2009) Nanoparticles, human health hazard and regulation. J R Soc Interface 7 (Suppl_1):S119–S129

Shabani KS, Ardejani FD, Badii K, Olya ME (2017) Preparation and characterization of novel nano-mineral for the removal of several heavy metals from aqueous solution: batch and continuous systems. Arab J Chem 10:S3108–S3127

Shah MMR, Liang Y, Cheng JJ, Daroch M (2016) Astaxanthin-Producing Green Microalga H. pluvialis: From Single Cell to High Value Commercial Products. Front Plant Sci; https://doi.org/10.3389/fpls.2016.00531

Solovchenko A, Solovchenko O, Khozin-Goldberg I, Didi-Cohen S, Pal D, Cohen Z et al. (2013) Probing the effects of high-light stress on pigment and lipid metabolism in nitrogen-starving microalgae by measuring chlorophyll fluorescence transients: studies with a Δ5 desaturase mutant of Parietochloris incisa (Chlorophyta, Trebouxiophyceae). Algal Res 2(3):175–182

Solovchenko AE (2015) Recent breakthroughs in the biology of astaxanthin accumulation by microalgal cell. Photosynth Res 125 (3):437–449

Sousa CA, Soares HM, Soares EV (2018) Toxic effects of nickel oxide (NiO) nanoparticles on the freshwater alga Pseudokirchneriella subcapitata. Aquat Toxicol 204:80–90

Sørensen SN, Engelbrekt C, Lützhøft HCH, Jiménez-Lamana J, Noori JS, Alatraktchi FA, Delgado CG, Slaveykova VI, Baun A (2016) A multimethod approach for investigating algal toxicity of platinum nanoparticles. Environ Sci Technol 50(19):10635–10643

Tayemeh MB, Esmailbeigi M, Shirdel I, Joo HS, Johari SA, Banan A, Nourani H, Mashhadi H, Jami MJ, Tabarrok M (2020) Perturbation of fatty acid composition, pigments, and growth indices of Chlorella vulgaris in response to silver ions and nanoparticles: a new holistic understanding of hidden ecotoxicological aspect of pollutants. Chemosphere 238:124576

Thomas NV, Kim S-K (2013) Beneficial effects of marine algal compounds in cosmeceuticals. Mar Drugs 11(1):146–164

Wang G, Hao Z, Huang Z, Chen L, Li X, Hu C et al. (2010) Raman spectroscopic analysis of a desert cyanobacterium Nostoc sp. in response to UVB radiation. Astrobiology 10(8):783–788

Wang F, Guan W, Xu L, Ding Z, Ma H, Ma A, Terry N (2019) Effects of nanoparticles on algae: adsorption, distribution, ecotoxicity and fate. Appl Sci 9(8):1534

Wang Z, Li J, Zhao J, Xing B (2011) Toxicity and internalization of CuO nanoparticles to prokaryotic alga microcystis aeruginosa as affected by dissolved organic matter. Environ Sci Technol 45(14):6032–6040

Wellburn AR (1994) The spectral determination of chlorophylls a and b, as well as total carotenoids, using various solvents with spectrophotometers of different resolution. J Plant Physiol 144(3):307–313

Zuo Z-J, Zhu Y-R, Bai Y-L, Wang Y (2012) Volatile communication between Chlamydomonas reinhardtii cells under salt stress. Biochem Syst Ecol 40:19–24